# Doubly excited $^{1,3}P^o$ resonance states of $Ps^-$ in weakly coupled plasmas

Sabyasachi Kar and Y. K. Ho
*Institute of Atomic and Molecular Sciences, Academia Sinica, P.O. Box 23-166, Taipei, Taiwan 106, Republic of China*
(Received 20 October 2005; published 2 March 2006)

The $^{1,3}P^o$ resonance states of positronium negative ions embedded in dense plasma environments are determined by calculating the density of resonance states using the stabilization method. A screened Coulomb potential obtained from the Debye model is used to represent the interaction between the charge particles, together with employing highly correlated wave functions to represent the correlation effect between them. We have calculated one $^1P^o$ and two $^3P^o$ resonances associated with and below the $n=2$ threshold of the positronium atom. The resonance energies and widths for various Debye lengths ranging from infinity to a small value are reported.

DOI: 10.1103/PhysRevA.73.032502 PACS number(s): 36.10.Dr, 34.80.Bm, 52.20.Fs

## I. INTRODUCTION

The study of atomic processes in dense plasma environments has been highlighted in several earlier investigations ([1–17] and references therein). These studies have been performed on the basis of the Debye screening concept. The concept of Debye screening has been derived from the weakly coupled classical plasmas for which the coupling constant is much smaller than unity. The effect of plasma is produced by the effective screening on the Coulomb potential. The Coulomb interaction plays an essential part in the determination of the system properties in plasmas in the sense that the cooperative effect stems from the long-range nature of the Coulomb potential. The Debye parameter is a function of the density and temperature of the charge particles. It is well known in the literature that the Debye-Hückel theory is a good approximation for certain specific conditions—for example, for low-density and high-temperature plasmas. There are several applications [18] of weakly coupled plasmas—for example, for gaseous-discharge plasmas, for plasma in controlled thermal nuclear fusion experiments, and for plasmas in solar corona. However, it is important to mention here that the main shortcoming of the Debye model is its limitation to static screening. For free $Ps^-$, there have been some experimental observations [19–22] and several theoretical investigations ([17,23–27] and references therein) are available in the literature. Recent interest in the resonances in free $Ps^-$ is shown in the works of Ivanov and Ho [24], Igarashi *et al.* [25], Papp *et al.* [26], and Li and Shakeshaft [27]. Recently, the ground-state energies [12,17] and the lowest $^1S^e$ resonances [17] of $Ps^-$ in plasmas for various Debye lengths have been reported. With the recent interest in free $Ps^-$ and with the recent development in the $^1S^e$ resonances of plasma-embedded $Ps^-$ [17], it is of great interest to investigate the $P$-state resonances of $Ps^-$ in plasma environments. We restrict ourselves in the static screened Coulomb potential to consider the plasma effect in the present calculations.

In the present work, we have investigated the $^{1,3}P^o$ resonances of the simplest three-lepton system $Ps^-$ in weakly coupled plasmas. To the best of our knowledge, no other investigation of $^{1,3}P^o$ resonance states of $Ps^-$ in the plasma environments has been reported in the literature. We have considered Debye screening to represent the interaction between charge particles. A correlated wave function involving the exponential expansion has been used to represent the correlation effect on the charge particles. One $^1P^o$ resonance and two $^3P^o$ resonances below the Ps ($n=2$) threshold are estimated by calculating the density of the resonance states using the stabilization method [28]. The convergence of the calculations has been examined with an increasing number of terms in the basis expansions. All the calculations were performed on DEC-ALPHA machines using quadruple-precision arithmetic (32 significant figures) in the UNIX environments. The atomic unit has been used throughout the work.

## II. THE METHOD

The nonrelativistic Hamiltonian describing the three-lepton system $(e^+,e^-,e^-)$ embedded in Debye plasmas characterized by the parameter $D$ is given by

$$H = -\frac{1}{2}\nabla_1^2 - \frac{1}{2}\nabla_2^2 - \frac{1}{2}\nabla_3^2 - \frac{\exp(-r_{31}/D)}{r_{31}} - \frac{\exp(-r_{32}/D)}{r_{32}} + \frac{\exp(-r_{12}/D)}{r_{12}}, \quad (1)$$

where 1, 2, and 3 denote the two electrons 1 and 2 and the positron, respectively, and $r_{ij}$ is the relative distance between particles $i$ and $j$. As the Debye parameter is a function of electron density ($n$) and electron temperature ($T$), various plasma conditions can be simulated for different choices of $n$ and $T$. The smaller values of $D$ are associated with stronger screening.

For the $^{1,3}P^o$ states of $Ps^-$, we have employed the wave function

$$\Psi = (1 + S_{pn}P_{12})\sum_{i=1}^{N} C_i r_{31}\cos\theta_1 \times \exp[(-\alpha_i r_{31} - \beta_i r_{32} - \gamma_i r_{21})\omega], \quad (2)$$

where $\alpha_i$, $\beta_i$, and $\gamma_i$ are the nonlinear variation parameters,

 

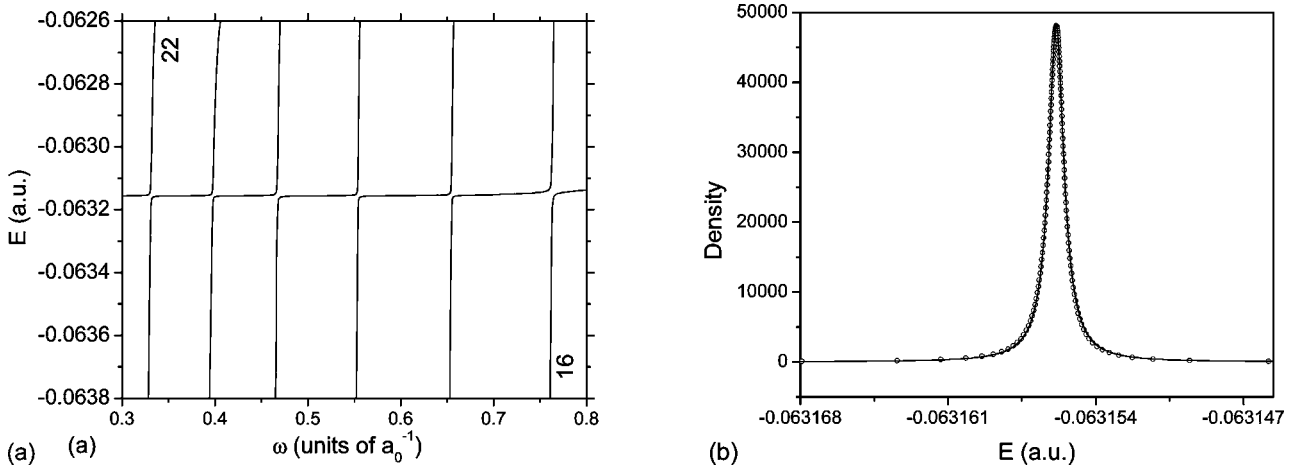


FIG. 1. (a) Stabilization plots for the lowest $^1P^o$ state of $Ps^-$ in Debye plasma for $D \to \infty$. (b) Calculated density (circles) and the best fitted Lorentzian form (solid line) corresponding to the lowest $^1P^o$ state of $Ps^-$ in Debye plasma for $D \to \infty$, for the 21st energy level in (a).

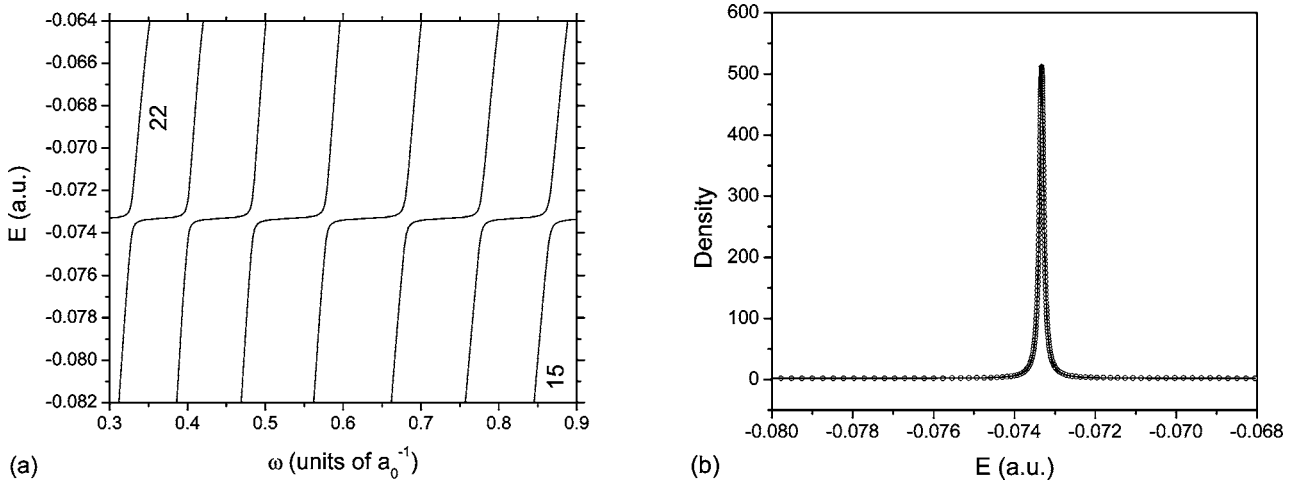


FIG. 2. (a) Stabilization plots for the lowest $^3P^o$ state of $Ps^-$ in Debye plasma for $D \to \infty$. (b) Calculated density (circles) and the best fitted Lorentzian form (solid line) corresponding to the lowest $^3P^o$ state of $Ps^-$ in Debye plasma for $D \to \infty$, for the 18th energy level in (a).

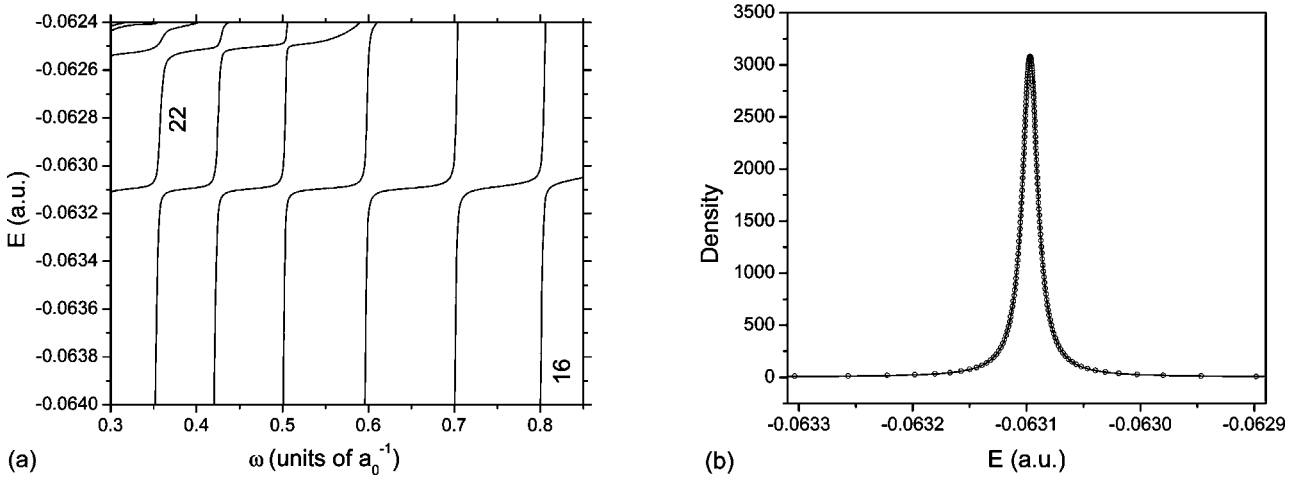


FIG. 3. (a) Stabilization plots for the $^3P^o(2)$ state of $Ps^-$ in Debye plasma for $D \to \infty$. (b) Calculated density (circles) and the best fitted Lorentzian form (solid line) corresponding to the $^3P^o(2)$ state of $Ps^-$ in Debye plasma for $D \to \infty$, for the 21st energy level in (a).

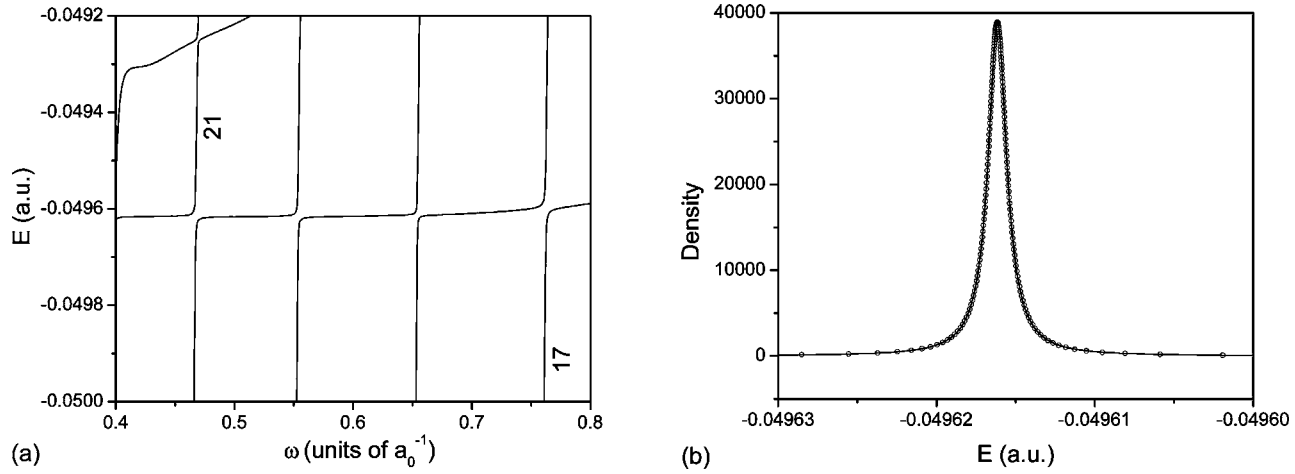


FIG. 4. (a) Stabilization plots for the lowest $^1P^o$ state of $Ps^-$ in Debye plasma environments for $D=70$. (b) Calculated density (circles) and the best fitted Lorentzian form (solid line) corresponding to the lowest $^1P^o$ state of $Ps^-$ for the 19th energy level in (a).

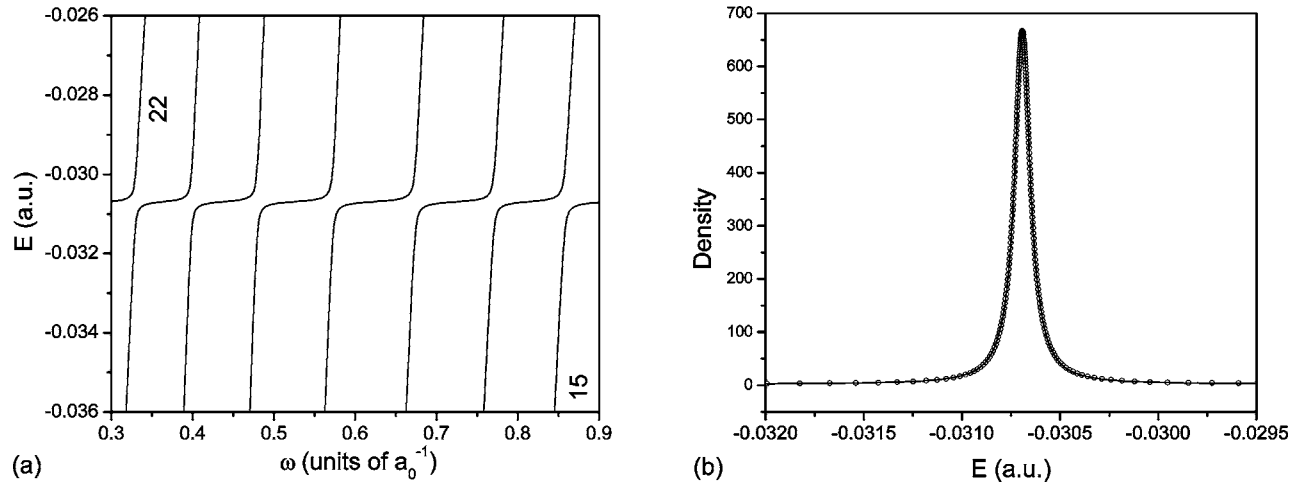


FIG. 5. (a) Stabilization plots for the $^3P^o(1)$ state of $Ps^-$ in Debye plasma environments for $D=20$. (b) Calculated density (circles) and the best fitted Lorentzian form (solid line) corresponding to the $^3P^o(1)$ state of $Ps^-$ for the 18th energy level in (a).

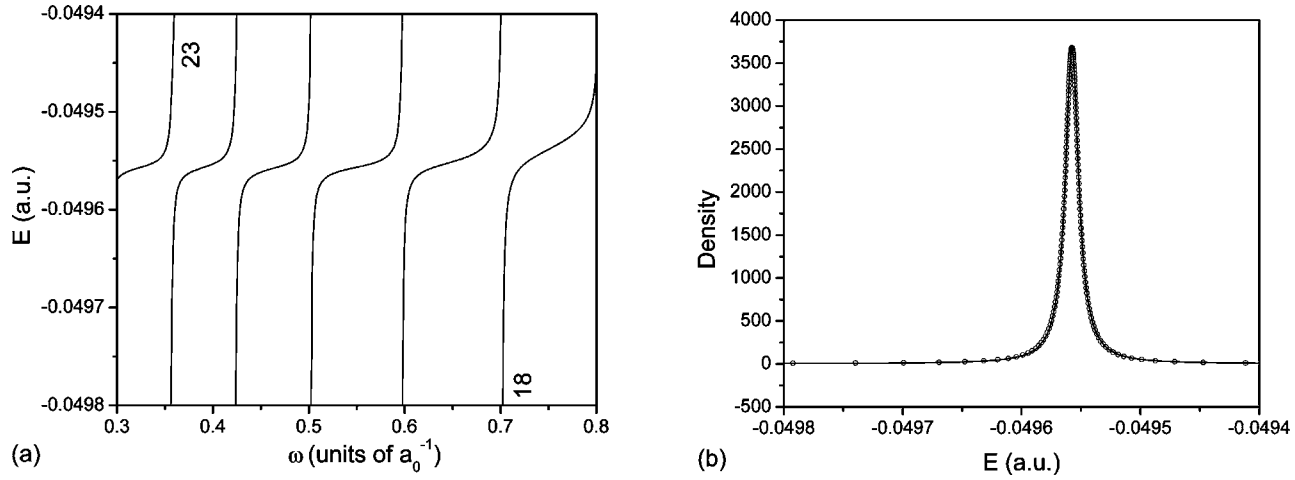


FIG. 6. (a) Stabilization plots for the $^3P^o(2)$ state of $Ps^-$ in Debye plasma environments for $D=70$. (b) Calculated density (circles) and the best fitted Lorentzian form (solid line) corresponding to the $^3P^o(2)$ state of $Ps^-$ for the 21st energy level in (a).

TABLE I. The convergence of the $^{1,3}P^o$ resonance energies ($E_r$) and widths ($\Gamma$) of $Ps^-$ in plasmas for different Debye lengths. The notation $a[-b]$ stands for a $a\times10^{-b}$. The quoted results are in atomic units.

| $D(a_0^{-1})$ | Resonance states | Resonance parameters | $N$ = 400 | $N$ = 500 | $N$ = 600 |
|---|---|---|---|---|---|
| $\infty$ | $^1P^o(1)$ | $-E_r$ | 0.06315544 | 0.06315586 | 0.06315588 |
| | | $\Gamma$ | 1.4[−6] | 1.07[−6] | 8.87[−7] |
| | $^3P^o(1)$ | $-E_r$ | 0.07332506 | 0.07332673 | 0.07332659 |
| | | $\Gamma$ | 1.283[−4] | 1.281[−4] | 1.274[−4] |
| | $^3P^o(2)$ | $-E_r$ | 0.0630958 | 0.0630969 | 0.0630970 |
| | | $\Gamma$ | 2.3[−5] | 1.61[−5] | 1.64[−5] |
| 70 | $^1P^o(1)$ | $-E_r$ | 0.0496157 | 0.04961562 | 0.0496161 |
| | | $\Gamma$ | 1.39[−6] | 1.36[−6] | 1.42[−6] |
| | $^3P^o(1)$ | $-E_r$ | 0.0595479 | 0.0595472 | 0.0595471 |
| | | $\Gamma$ | 1.259[−4] | 1.266[−4] | 1.259[−4] |
| | $^3P^o(2)$ | $-E_r$ | 0.0495559 | 0.0495562 | 0.0495575 |
| | | $\Gamma$ | 1.50[−5] | 1.35[−5] | 1.35[−5] |
| 20 | $^1P^o(1)$ | $-E_r$ | 0.02470 | 0.02476 | 0.02482 |
| | $^3P^o(1)$ | $-E_r$ | 0.0306907 | 0.0306922 | 0.0306920 |
| | | $\Gamma$ | 9.72[−5] | 9.71[−5] | 9.70[−5] |
| | $^3P^o(2)$ | $-E_r$ | 0.02482 | 0.02482 | 0.02486 |

$C_i$ $(i=1,\ldots,N)$ are the linear expansion coefficients, $N$ is the number of basis terms, $S_{pn}=1$ indicates singlet states and $S_{pn}=-1$ assigns triplet states, $\omega$ is a scaling constant to be discussed later in the text, and $P_{12}$ is the permutation operator defined by $P_{12}f(r_{31},r_{32},r_{12},\theta_1)=f(r_{32},r_{31},r_{12},\theta_2)$. We have used the same values of the nonlinear variation parameters $\alpha_i$, $\beta_i$, and $\gamma_i$ chosen from a quasirandom process [29] and as used in our earlier work [17] for calculations of the ground state and resonance state of plasma-embedded $Ps^-$. In our earlier work [17], the exponential part of the wave function (2) should be read as $\exp[(-\alpha_i r_{31}-\beta_i r_{32}-\gamma_i r_{21})\omega]$. The necessary integrals involving the screened Coulomb potential for the evaluation of the necessary matrix elements are discussed in the literature ([10] and references therein).

## III. RESULTS AND DISCUSSION

The stabilization method has been used to extract resonance energies and widths by calculating the density of resonance states. The energy levels $E(\omega)$ have been calculated by diagonalizing the Hamiltonian (1) using the basis functions (2) with different $\omega$ values. After constructing a stabilization diagram by plotting the energy levels $E(\omega)$ versus $\omega$, the resonance position can be identified by observing the slowly decreasing eigenenergy in the stabilization plateau. The scaling parameter $\omega$ in the wave function [Eq. (2)] can be considered as the reciprocal range of a "soft" wall [30]. Detailed discussions are available in the works of Ho and co-workers [15,17,30,31]. Varying the Debye length $D$ from infinity to small values, different resonance parameters (energy and width) have been obtained.

To extract the resonance energy $E_r$ and the resonance width $\Gamma$, we have calculated the density of the resonance states for a single energy level with the help of the formula

$$\rho_n(E)=\left|\frac{E_n(\omega_{i+1})-E_n(\omega_{i-1})}{\omega_{i+1}-\omega_{i-1}}\right|^{-1}_{E_n(\omega_i)=E}, \tag{3}$$

where the index $i$ is the $i$th value for $\omega$ and the index $n$ is for the $n$th resonance. After calculating the density of resonance states $\rho_n(E)$ with the above formula (3), we fit it to the following Lorentzian form that yields resonance energy $E_r$ and total width $\Gamma$:

$$\rho_n(E)=y_0+\frac{A}{\pi}\frac{\Gamma/2}{(E-E_r)^2+(\Gamma/2)^2}, \tag{4}$$

where $y_0$ is the base-line offset, $A$ is the total area under the curve from the base line, $E_r$ is the center of the peak, and $\Gamma$ denotes the full width of the peak of the curve at half height.

The single Lorentzian fitting formula (4) is a multiparameter fitting function corresponding to the Briet-Wigner resonance formula. It has been investigated in the works of Fang and Ho [32] that the single Lorentzian fitting formula (4) works for strongly overlapping resonances. It is also interesting to mention here that Müller *et al.* [33] have used the stabilization method to calculate the isolated as well as overlapping resonances of helium. We have mentioned $\rho_n(E)$ as the density of resonance state, whereas in an analytical study of Bowman [34] from the collisional point of view, a similar type of states is referred to as the "density of resonances" obtain from a certain resonant part of the cumulative lifetime.

To construct the stabilization plot, we have used expansion length of $N=600$ in the basis function (2). We have calculated energy levels as a function of $\omega$ in a range from 0.3 to 1.0. The stabilization diagrams [in Figs. 1(a), 2(a), and

TABLE II. The $^{1,3}P^o$ resonance energies and widths of $Ps^-$ in plasmas for various Debye lengths along with the Ps(2*S*) threshold energies $E_{Ps(2S)}$. The notation $a[-b]$ stands for a $a\times10^{-b}$. The quoted results are in atomic units.

| $D(a_0^{-1})$ | Resonance parameters | $^1P^o(1)$ | $^3P^o(1)$ | $^3P^o(2)$ | $-E_{Ps(2S)}$ |
|---|---|---|---|---|---|
| $\infty$ | $-E_r$ | 0.0631559<br>0.0631553[a]<br>0.063155[b] | 0.07332659<br>0.07332735[a] | 0.063097<br>0.063097[a] | 0.062500 |
| | $\Gamma$ | 8.87[−7]<br>1.0[−6][a]<br>9.92[−7][b] | 1.274[−4]<br>1.278[−4][a] | 1.64[−5]<br>1.6[−5][a] | |
| 200 | $-E_r$ | 0.0582334 | 0.06838366 | 0.058173 | 0.0576466 |
| | $\Gamma$ | 9.58[−7] | 1.273[−4] | 1.61[−5] | |
| 100 | $-E_r$ | 0.053499 | 0.06356607 | 0.053437 | 0.0530742 |
| | $\Gamma$ | 1.31[−6] | 1.268[−4] | 1.51[−5] | |
| 70 | $-E_r$ | 0.0496161 | 0.0595471 | 0.049557 | 0.0493657 |
| | $\Gamma$ | 1.42[−6] | 1.259[−4] | 1.35[−5] | |
| 60 | $-E_r$ | 0.047535 | 0.0573612 | 0.047482 | 0.0473860 |
| | $\Gamma$ | 1.5[−6] | 1.25[−4] | 1.23[−5] | |
| 50 | $-E_r$ | 0.044723 | 0.0543595 | 0.044686 | 0.0447073 |
| | $\Gamma$ | | 1.24[−4] | 0.00001 | |
| 40 | $-E_r$ | 0.04078 | 0.0499896 | 0.04079 | 0.0408856 |
| | $\Gamma$ | | 1.21[−4] | | |
| 30 | $-E_r$ | 0.03489 | 0.0430748 | 0.03491 | 0.0350118 |
| | $\Gamma$ | | 1.15[−4] | | |
| 25 | $-E_r$ | 0.0306 | 0.037886 | 0.0306 | 0.0307323 |
| | $\Gamma$ | | 1.09[−4] | | |
| 20 | $-E_r$ | 0.0248 | 0.0306920 | 0.0249 | 0.0249641 |
| | $\Gamma$ | | 9.70[−5] | | |
| 15 | $-E_r$ | 0.0168 | 0.020313 | 0.017 | 0.0169025 |
| | $\Gamma$ | | 7.23[−5] | | |
| 10 | $-E_r$ | 0.0059 | 0.00602 | | 0.00605257 |
| | $\Gamma$ | | 1.4[−5] | | |

[a]Bhatia and Ho [23].
[b]Igarashi *et al.* [25].

3(a)] corresponding to the Debye length $D$ tending to $\infty$ (a.u.) show the stabilization character near $E=-0.063$, $-0.073$, and $-0.063$ a.u., respectively, for the $^1P^o(1)$, $^3P^o(1)$, and $^3P^o(2)$ resonance states. For each of the spin cases, we use 1401 points to cover the range of $\omega$ from 0.3 to 1.0 in a mesh size of 0.0005. We then calculate the density of resonance states for the individual energy levels in the range $\omega=0.3-1.0$, with one energy level at a time. The calculated density of resonance states from the single energy eigenvalue is then fitted to Eq. (4), and the one that gives the best fit (with the least $\chi$ square and with the square of the correlation coefficient much closer to 1) to the Lorentzian form is considered as the desired results for that particular resonance. Figures 1(b), 2(b), and 3(b) show the fitting of the density of the resonance states for the 21st, 18th, and 21st eigenvalues of the stabilization plot in Figs. 1(a), 2(a), and 3(a), respectively. From the fits, we obtain the resonance parameters $(E_r,\Gamma)$ in the unscreened case as $(-0.063\,155\,88, 8.87\times10^{-7})$ for the $^1P^o(1)$ state, $(-0.073\,326\,59, 1.274\times10^{-4})$ for the $^3P^o(1)$ state, and $(-0.063\,096\,96, 1.64\times10^{-5})$ for the $^3P^o(2)$ state. The resonance energy and width are nicely comparable with the reported results of Bhatia and Ho [23] and of Igarashi *et al.* [25]. The circles are the results of the actual calculations of the density of the resonance states using formula (3), and the solid line is the fitted Lorentzian form of the corresponding $\rho_n(E)$. The stabilization plots in Figs. 4(a), 5(a), and 6(a) correspond to the $^1P^o(1)$ state for $D=70$, the $^3P^o(1)$ state for $D=20$, and the $^3P^o(2)$ state for $D=70$, respectively. They show the stabilization character near the energy $E=-0.05$, $-0.031$, and $-0.05$ (a.u.). Figures 4(b), 5(b), and 6(b) show the fittings of the density of the resonance states for the 19th, 18th, and 21st eigenvalues, respectively, corresponding to the stabilization plots 4(a), 5(a), and 6(a). The best values of the resonances parameters have been obtained from the 19th energy level for the $^1P^o(1)$ state except for the unscreened case and for $D=200$, the 18th energy level for the $^3P^o(1)$ state, and the 21st energy level for the $^3P^o(2)$ state.

Table I shows the convergence of the resonance energies and the widths for $N=400$, 500, and 600 basis terms corresponding to $D=20$, 70, and infinity. It has been mentioned earlier in Sec. II that we have used the same parameters in

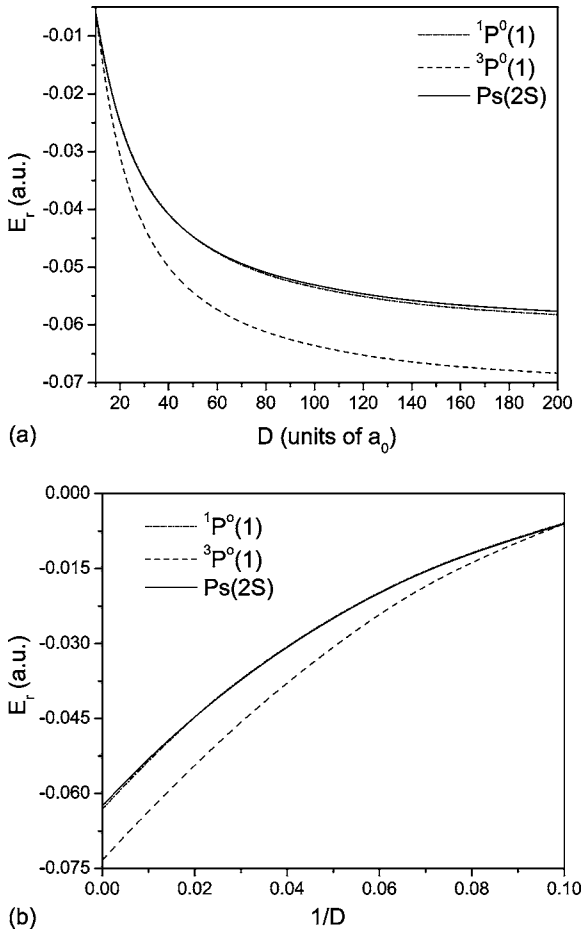


FIG. 7. The $^{1,3}P^o(1)$ resonances energies in terms of Debye length $D$ in (a) and in terms of Debye parameter $1/D$ in (b) along with the Ps($2S$) threshold energies (solid line).

the present work as used in our earlier $^1S^e$ state of plasma-embedded $Ps^-$ calculations [17]. It is seen from Table I that the convergence of the resonance energies and widths are quite good. Table II presents the resonance energies and widths for the various Debye lengths ranging from infinity (corresponding to no screening) to a small value 10 (corresponding to strong screening) along with Ps ($2S$) threshold energies. In Table II, we have compared our results in the unscreened case with the reported results of Bhatia and Ho [23] and of Igarashi *et al.* [25]. The results of Ps($2S$) threshold energies are taken from the earlier calculations (Kar and Ho [31]).

All the results shown in Figs. 1–10 and Table II are obtained using the 600-term wave functions. Our calculated $^{1,3}P^o(1)$ resonances associated with and below the Ps($n=2$) threshold are shown in Fig. 7 along with the Ps($2S$) threshold energies for the different values of $D$ and $1/D$, respectively, with the corresponding widths plotted in Figs. 8 and 9. We have not included our calculated $^3P^o(2)$ resonance energies in Fig. 7 as these energies are close to the $^1P^o(1)$ states. For the $^3P^o(2)$ resonance states, the widths are plotted in Fig. 10 in terms of the Debye length $D$ and in terms of the Debye parameter $1/D$.

It is clear from Figs. 8–10 and Table II that the $^1P^o(1)$ resonance widths increase with increasing plasma strength whereas the $^3P^o$ resonance widths decrease with an increase of plasma strength. We have obtained the $^1P^o(1)$ resonance widths up to $D=60$, the $^3P^o(1)$ resonance widths up to $D=10$, and the $^3P^o(1)$ resonance widths up to $D=50$. It is apparent from Table II and Fig. 7(a) that the $^1P^o(1)$ and $^3P^o(2)$ resonance energies are lying above the Ps($2S$) threshold energies for the value of Debye length $D$ around 50 [consequently for the value of the Debye parameter $1/D$ around 0.02 in Fig. 7(b)]. The $^1P^o(1)$ resonance energy crosses the $^3P^o(2)$ resonance energy at $D=25$, and the $^1P^o(1)$ resonance energies are lying above the $^3P^o(2)$ resonance energies for the values of $D$ less than 25. The resonances obtained below the Ps($2S$) threshold correspond to Feshbach resonances (below threshold) and the resonances obtained above the Ps($2S$) threshold correspond to shape resonances (above threshold). For the $^1P^o(1)$ state, Feshbach resonances occur for values of $D$ grater than 50 and shape resonances occur for $D$ less than 50. For the $^3P^o(2)$ state, Feshbach resonances occur for values of $D$ grater than 60 and shape resonances occur for $D$ less than 60.

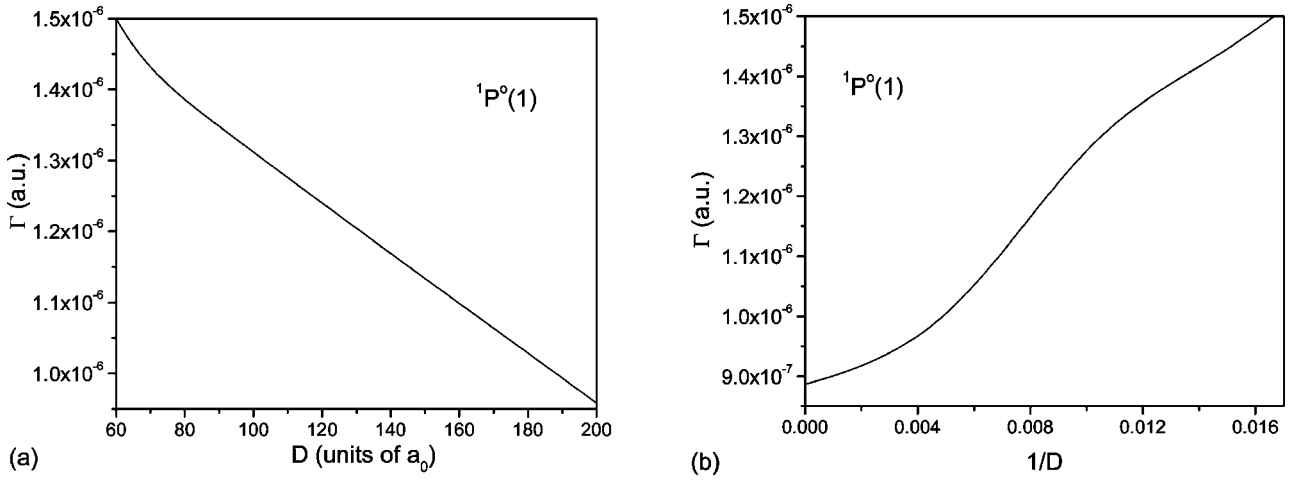


FIG. 8. The $^1P^o(1)$ resonances widths in terms of Debye length $D$ in (a) and in terms of Debye parameter $1/D$ in (b) corresponding to resonance energies in Fig. 7.

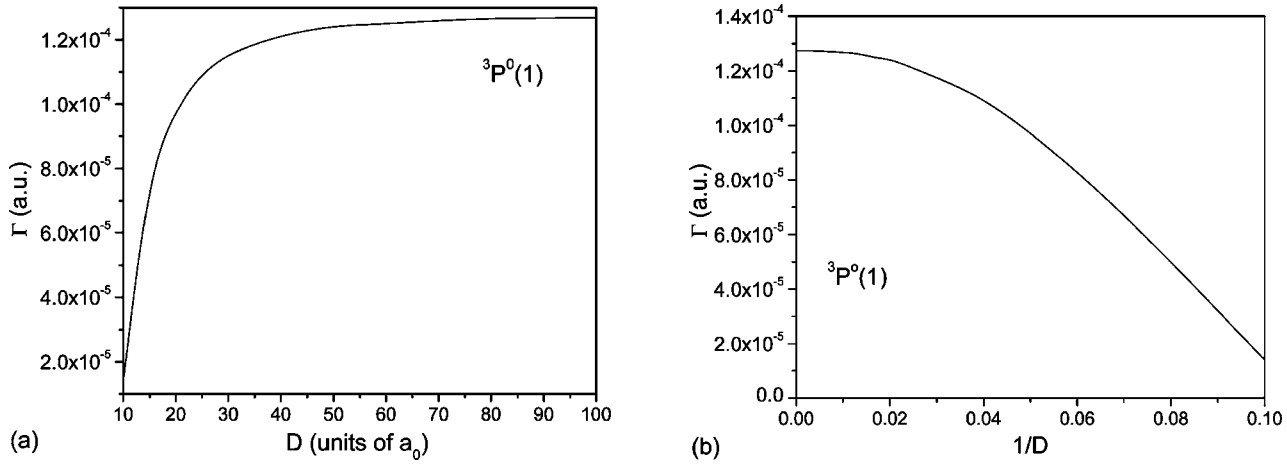


FIG. 9. The $^3P^o(1)$ resonances widths in terms of Debye length $D$ in (a) and in terms of Debye parameter $1/D$ in (b) corresponding to resonance energies in Fig. 7.

From Figs. 9 and 10 and Table II, it is seen that the resonance widths $\Gamma$ for the two $^3P^o$ states decreases with decreasing value of $D$ (with increasing $1/D$). The situation can be explained in the following way: The $^3P^o$ states in $Ps^-$ are "+" states, and the two electrons are located on opposite sides of the positron. The movements of the two electrons are moving toward the positron "in phase." The autoionization of such a state is through the momentum transfer, as one of the electrons is "knocked out" by the other via the positron. Apparently, when the electron-positron screening is increased (decreasing $D$, increasing $1/D$), the movement of the electrons will be slowed down. As a result, the lifetime of the autoionization process will be prolonged, leading to a narrowing of the resonance width, a consequence of the uncertainty principle.

From Fig. 8 and Table II, it is apparent that the resonance width $\Gamma$ for the $^1P^o$ state increases with decreasing value of $D$ (with increasing $1/D$). The situation can be explained in the following way: The $^1P^o$ state in $Ps^-$ is a "−" state [35], and one of the electrons is located further away from the excited positronium. The interaction between the outer electron and the "parent positronium" is an attractive dipole potential of order $r^{-2}$. When such a quasibound state interacts with the scattering continuum the outer electron would autoionize. When the screening effect increases (increasing $1/D$), the strength of the attractive dipole potential will diminish and the outer electron hence autoionize more rapidly, leading to a broadening of the resonance width, a result from again the uncertainty principle.

It should be mentioned here that we have calculated the $^{1,3}P^o(1)$ resonances up to $D=10$ and the $^3P^o(2)$ resonance up to $D=15$. If the $^1P^o(1)$ [or $^3P^o(2)$] resonances were to exist for $D\leqslant 9$ [or $D<15$], it would be shape resonances. If the $^3P^o(1)$ resonances were to exist for $D\leqslant 9$, it would be located at a region very near to the $Ps(2S)$ threshold. However, calculations for such resonances would require more extensive basis sets in the wave functions, and no attempt is made to carry out large-scale calculations here.

We next discuss the possible decay routes for the doubly excited states of $Ps^-$.

(I) Autoionization: the doubly excited state, denoted by $(Ps^-)^{**}$, may decay to the ground state of Ps by ejecting an electron. The process is called autoionization:

$$(Ps^-)^{**}(2snp\ ^{1,3}P^o) \rightarrow Ps(1S) + e^-. \tag{5}$$

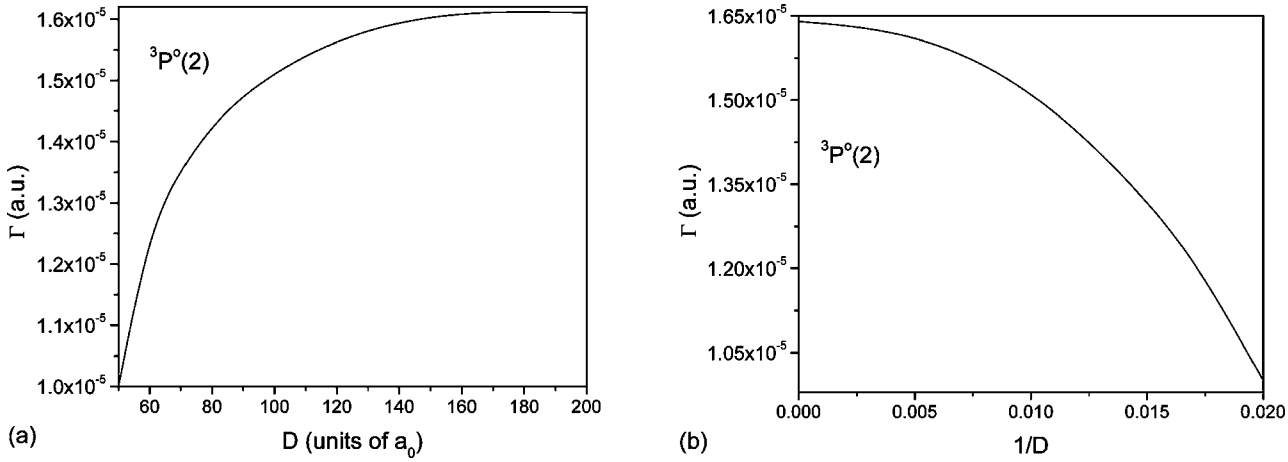


FIG. 10. The $^3P^o(2)$ resonances widths in terms of Debye length $D$ in (a) and in terms of Debye parameter $1/D$ in (b).

For the present case the $^{1,3}P^o$ states lie below the Ps($n$=2) thresholds, there is only one open channel, and the widths we have reported here are the "total widths" as far as the autoionization processes is concerned.

(II) Radiative decay: for the singlet-spin state, the system may cascade to the ground state of $Ps^-$,

$$(Ps^-)^{**}(2s3p\ ^1P^o) \rightarrow (Ps^-)^{**}(1s^2\ ^1S^e) + \hbar\omega, \tag{6}$$

by emitting a photon. Alternatively, it may cascade to a lower-lying $S$-wave doubly excited state—i.e.,

$$(Ps^-)^{**}(2s3p\ ^1P^o) \rightarrow (Ps^-)^{**}(2s^2\ ^1S^e) + \hbar\omega. \tag{7}$$

For the triplet-spin case, the system may cascade to an $S$-wave doubly excited state—i.e.,

$$(Ps^-)^{**}(2s2p\ ^3P^o) \rightarrow (Ps^-)^{**}(2s3s\ ^3S^e) + \hbar\omega. \tag{8}$$

The processes described in Eqs. (7) and (8) are very similar to the "dielectronic recombination" for electron-ion collisions in atomic cases. Without the plasma environments ($D \rightarrow \infty$), for a resonance with a "not-extremely-narrow" width, the autoionization rate usually is much larger than the radiative rates for low-$Z$ ions.

(III) Annihilation: a unique decay route for atomic systems involving positrons is that the positron may annihilate with one of the electrons. For $Ps^-$, the positron and an electron annihilate with each other, leaving one electron behind,

$$(Ps^-)^{**} \rightarrow n\gamma + e^-. \tag{9}$$

Usually, the two-photon case ($n$=2) would be the dominate annihilation process. However, the one-photon, three-photon, etc., processes are also possible, but with considerably smaller rates. In an earlier study [36] of two-photon annihilation for the doubly excited $^1S^e$ states in $Ps^-$ (again without the plasma environments), it was found that the autoionization rates are much larger than the annihilation rates. Even for a narrow resonance such as the 2s3s $^1S^e$ state, the autoionization rate is about 3000 times lager than the annihilation rate. Here we assume that for the $P$ waves, the autoionization would still be the dominant process.

The above discussion is valid for the unscreened ($D \rightarrow \infty$) positronium ions. The situation may change when the $Ps^-$ ion is embedded in a plasma, as the radiatively decay line may be broadened and shifted by the plasma effect. The subject of line shifts and broadening is an active research area in plasma physics [37]. However, while there has been considerable among of work for bound singly excited states, investigations of the line broadening for doubly excited states are very scared. As we have predicted that the autoionization width would decrease for some states (i.e., the $^3P^o$ states) when the screening effect increases (increasing $1/D$), the radiative decay may become more competitive as the decay line is broadened for increasing plasma effect. As for positron annihilation in plasma environments, again to the best of our knowledge, no such investigation has been reported in the literature. Overall, the above three decay processes are competing, and interfering, with each other. The autoionization widths we have reported here represent partial widths as far as the overall decay is concerned. In the present work, we have not considered the radiative decay process and the positron annihilation process. Studies of such processes for doubly excited positronium ions are of interest, and it is worthwhile for future investigations. Our present work is a first step to shed light on an intriguing problem involving doubly excited positronium ions embedded in plasmas.

Finally, we should also mention that we have not considered another possible decay route for the $(Ps^-)^{**}$ when one of the electrons in $Ps^-$ is lost to "recombination" by collisions with a positively charged ion (denoted by $A^+$) in the plasma,

$$(Ps^-)^{**} + A^+ \rightarrow Ps + A. \tag{10}$$

For a weakly coupled plasma in which the number density of $A^+$ ions is low, we assume that the recombination rate in the process (10) is small, and we have not considered such a process in the present investigation.

## IV. CONCLUSIONS

This work presents a calculation on the doubly excited $^{1,3}P^o$ resonance states of positronium negative ions embedded in weakly coupled plasma environments. One-$^1P^o$-state and two-$^3P^o$-state resonance energies and widths for the various Debye parameters ranging from infinity to small value (up to 10) have been reported. We have also obtained the range of values of the Debye length for the identification of the appearance of the Feshbach to shape resonances for the $^1P^o(1)$ and $^3P^o(2)$ states. The stabilization method is used to extract resonance energies and widths. This method is a practical method to calculate resonance parameters $(E_r, \Gamma)$ as only the real algorithm is used throughout the entire calculation. Our present work will provide useful information to the plasma physics research community, as well as to the positron physics community, which is interested in such a three-lepton system. Finally we should mention here that the Debye-Hückel theory is a good approximation for weakly coupled plasmas in the high-temperature and low-density limit [38] whereas the ion-sphere model is the better approximation for strongly coupled plasmas in the low-temperature and high-density limit [38]. But the study of plasma-embedded atoms using an ion-sphere potential is outside the scope of our present investigation.

## ACKNOWLEDGMENT

This work is supported by the National Science Council of R.O.C.

[1] F. J. Rogers, H. C. Grabsoke, Jr., and D. J. Harwood, Phys. Rev. A **1**, 1577 (1970).
[2] K. M. Roussel and R. F. O'Connell, Phys. Rev. A **9**, 52 (1974).
[3] C. S. Lam and Y. P. Varshni, Phys. Rev. A **27**, 418 (1983).
[4] T. Hashino, S. Nakazaki, T. Kato, and H. Kashiwabara, Phys. Lett. A **123**, 236 (1987).
[5] Z. Wang and P. Winkler, Phys. Rev. A **52**, 216 (1995).
[6] L. Zhang and P. Winkler, Int. J. Quantum Chem., Quantum Chem. Symp. **30**, 1643 (1996).
[7] P. Winkler, Phys. Rev. E **53**, 5517 (1996).
[8] X. Lopez, C. Sarasola, and J. M. Ugalde, J. Phys. Chem. A **101**, 1804 (1997).
[9] J. M. Mercero, J. E. Fowler, C. Sarasola, and J. M. Ugalde, Phys. Rev. A **57**, 2550 (1998).
[10] S.-T. Dai, A. Solovyova, and P. Winkler, Phys. Rev. E **64**, 016408 (2001).
[11] B. Saha, T. K. Mukherjee, P. K. Mukherjee, and G. H. F. Diercksen, Theor. Chem. Acc. **108**, 305 (2002).
[12] B. Saha, T. K. Mukherjee, and P. K. Mukherjee, Chem. Phys. Lett. **373**, 218 (2003).
[13] A. N. Sil and P. K. Mukherjee, Int. J. Quantum Chem. **102**, 1061 (2004).
[14] L. B. Zhao and Y. K. Ho, Phys. Plasmas **11**, 1695 (2004).
[15] S. Kar and Y. K. Ho, Phys. Rev. E **70**, 066411 (2004); Chem. Phys. Lett. **402**, 544 (2005); New J. Phys. **7**, 141 (2005); Phys. Rev. A **72**, 010703(R) (2005); J. Phys. B **38**, 3299 (2005); Int. J. Quantum Chem. **106**, 814 (2006).
[16] H. Okutsu, T. Sako, K. Yamanouchi, and G. H. F. Diercksen, J. Phys. B **38**, 917 (2005).
[17] S. Kar and Y. K. Ho, Phys. Rev. A **71**, 052503 (2005).
[18] S. Ichimaru, in *Plasma Physics* (Benjamin/Cummings, Menlo Park, CA, 1986), pp. 5–10.
[19] Allen Paine Mills, Jr., Phys. Rev. Lett. **46**, 717 (1981).
[20] Allen Paine Mills, Jr., Phys. Rev. Lett. **50**, 671 (1983).
[21] D. Schwalm, F. Fleischer, M. Lestinsky, K. Degreif, G. Gwinner, V. Liechtenstein, F. Plenge, and H. Scheit, Nucl. Instrum. Methods Phys. Res. B **221**, 185 (2004).
[22] P. Balling, D. Fregenal, T. Ichioka, H. Knudsen, H.-P. E. Kristiansen, J. Merrison, and U. Uggerhøj, Nucl. Instrum. Methods Phys. Res. B **221**, 200 (2004).
[23] Y. K. Ho, Phys. Rev. A **19**, 2347 (1979); A. K. Bhatia and Y. K. Ho, *ibid.* **42**, 1119 (1990); Y. K. Ho and A. K. Bhatia, *ibid.* **44**, 2890 (1991).
[24] Y. K. Ho, Chin. J. Phys. **35**, 2347 (1997); I. A. Ivanov and Y. K. Ho, Phys. Rev. A **60**, 1015 (1999); **61**, 32501 (2000).
[25] A. Igarashi, I. Shimamura, and N. Toshima, New J. Phys. **2**, 17 (2000).
[26] Z. Papp, C.-Y. Hu, Z. T. Hlousek, B. Konya, and S. L. Yakolev, Phys. Rev. A **63**, 062721 (2001); Z. Papp, J. Darai, C.-Y. Hu, Z. T. Hlousek, B. Konya, and S. L. Yakolev, *ibid.* **65**, 032725 (2002).
[27] T. Li and R. Shakeshaft, Phys. Rev. A **71**, 052505 (2005).
[28] V. A. Mandelshtam, T. R. Ravuri, and H. S. Taylor, Phys. Rev. Lett. **70**, 1932 (1993).
[29] A. M. Frolov, Phys. Rev. E **64**, 036704 (2001).
[30] S. Kar and Y. K. Ho, J. Phys. B **37**, 3177 (2004).
[31] S. Kar and Y. K. Ho, J. Phys. B **38**, 3299 (2005); Eur. Phys. J. D **35**, 453 (2005); U. Roy and Y. K. Ho, J. Phys. B **35**, 2149 (2002); Nucl. Instrum. Methods Phys. Res. B **221**, 36 (2004); Z.-C. Yan and Y. K. Ho, J. Phys. B **36**, 4417 (2003); T. K. Fang and Y. K. Ho, *ibid.* **32**, 3863 (1999); W. J. Pong and Y. K. Ho, *ibid.* **31**, 2177 (1998); S. S. Tan and Y. K. Ho, Chin. J. Phys. **35**, 701 (1997).
[32] T. K. Fang and Y. K. Ho, J. Phys. B **32**, 3863 (1999).
[33] J. Müller, X. Yang, and J. Burgdörfer, Phys. Rev. A **49**, 2470 (1994).
[34] J. M. Bowman, J. Phys. Chem. **90**, 3492 (1986).
[35] J. Botero and C. H. Greene, Phys. Rev. Lett. **56**, 1366 (1986); J. Botero, Phys. Rev. A **35**, 36 (1987).
[36] Y. K. Ho, Phys. Rev. A **32**, 2501 (1985).
[37] H. R. Griem, *Spectral Line Broadening by Plasmas* (Academic, New York, 1974).
[38] B. L. Whitten, N. F. Lane, and J. C. Weisheit, Phys. Rev. A **29**, 945 (1984).